



An ALD aluminum oxide passivated Surface Acoustic Wave sensor for early biofilm detection

Young Wook Kim^{a,b,*}, Saeed Esmaili Sardari^b, Mariana T. Meyer^{a,c}, Agis A. Iliadis^b, Hsuan Chen Wu^c, William E. Bentley^c, Reza Ghodssi^{a,b,c}

^a MEMS Sensors and Actuators Laboratory, Institute for Systems Research, University of Maryland, College Park, MD 20742, USA

^b Department of Electrical and Computer Engineering, University of Maryland, College Park, MD 20742, USA

^c Fischell Department of Bioengineering, University of Maryland, College Park, MD 20742, USA

ARTICLE INFO

Article history:

Received 8 July 2011

Received in revised form 3 January 2012

Accepted 7 January 2012

Available online 16 January 2012

Keywords:

Bacterial biofilm
Surface Acoustic Wave
ZnO passivation
Aluminum oxide
Atomic layer deposition
Fetal Bovine Serum

ABSTRACT

We present a successful demonstration of a reusable Surface Acoustic Wave (SAW) sensor for bacterial biofilm growth monitoring in an animal serum and bacterial growth media. Bacterial biofilms produce harmful metabolic by-products and are a characteristic of severe infections. Thus, continuous monitoring of bacterial biofilm growth is critical. Here, we report a highly sensitive SAW sensor for biofilm growth monitoring fabricated by depositing zinc oxide (ZnO) piezoelectric thin film by pulsed laser deposition (PLD). To prevent ZnO damage from long term exposure to bacterial growth media or to an animal serum, the ZnO layer of the sensor was effectively protected by aluminum oxide (Al₂O₃) using atomic layer deposition (ALD). As a result, the sensor was reusable for consecutive biofilm formation experiments. The detection limit of the SAW sensor was approximately 5.3 pg. The SAW sensor was tested with *Escherichia coli* W3110 in Lysogeny Broth (LB) media, and in 10% diluted Fetal Bovine Serum (FBS) as an approximation to an *in vivo* environment. The resonant frequency shift measured at the output of the SAW sensor in both LB media and 10% FBS corresponded to natural biofilm growth. These repeatable results support the novel application of a SAW sensor for real time biofilm sensing.

© 2012 Elsevier B.V. All rights reserved.

1. Introduction

Bacteria can attach to surfaces and form microcolonies as their population increases. The colonies eventually can form a community known as a bacterial biofilm [1,2]. A biofilm is not simply a group of bacteria, but a complex collection of microorganisms encased in an extracellular matrix. The extracellular matrix is composed of exopolysaccharideglycocalyx polymers which promote irreversible adhesion of microcolonies on the surface and also prevent diffusion of antibiotics through the biofilm [1,2]. Due to the complex extracellular matrix and heterogeneous bacterial composition, biofilms are resistant to bacteriophages in industry and to chemically diverse antibiotic treatments in clinical fields [3]. In addition, bacterial corrosion of metals is an economically important consequence of bacterial biofilm formation that illustrates several fascinating aspects of the structure and physiology of these adherent bacterial populations. Therefore, environmental, clinical, and industrial long term reliable biofilm growth monitoring is critical

to prevent contamination, severe infection, and corrosive problems due to the biofilm formation.

The measurement of bacterial biofilms with capacitive sensing has been applied by Yang and Li to monitor *Salmonella typhimurium* bacteria [4], and by Ghafar-Zadeh et al. to detect *Escherichia coli* (*E. coli*) [5]. In Yang and Li [4], an interdigitated microelectrode was fabricated to provide detectable impedance signals in capacitance measurement during bacterial growth. *S. typhimurium* bacteria were grown over the microelectrode and the capacitance change was continuously measured. Capacitive sensing in a liquid environment, however, can be interfered with by a conductive media due to the current flow through the growth media [4].

The direct impedance measurement of the attachment of *E. coli* on an electrode is demonstrated by other groups [6,7]. The change of impedance during bacterial growth is correlated with the biomass adhere on the electrode. This impedimetric sensing is particularly useful in detecting very early attachment of bacteria based on the significant impedance change observed upon attachment. However, long-term real-time biofilm monitoring by impedance measurement requires a continuous current source for bacterial detection which may cause interruption of bacterial growth.

* Corresponding author at: University of Maryland, 2201 JMP Building, College Park, MD 20742, USA. Tel.: +1 301 405 1897; fax: +1 301 314 9920.

E-mail addresses: ywkim@umd.edu (Y.W. Kim), ghodssi@umd.edu (R. Ghodssi).

Fluorescent methods have reported high sensitivity [8], but require fluorescent molecule labeling for sensing to occur. Labeling requires additional sample preparation and the fluorescent molecule can be degraded over long term exposure to liquid.

Electrochemical sensing can be used for selective detection a molecule without fluorescent labeling [9]. An electrochemical sensor array was integrated with a miniaturized bioreactor system for high throughput cell cultivation in 96 well plates [10]. Using a 100 μl working volume in the 96 well micro reactors, the sensor array can monitor temperature, pH, and oxygen concentration as well as total biomass. However, electrochemical sensors require a continuous power source for the operation and also require recalibration of the sensor due to the conductivity change of bacterial growth media in long term biofilm growth experiments.

Surface Acoustic Wave (SAW) sensors exhibit several advantages in small molecule detection including high sensitivity [11–22] and low power consumption [23]. A SAW sensor can detect mass or viscosity change due to the wave velocity attenuation, resulting in a resonant frequency shift at the output. A highly sensitive SAW sensor for detection of interleukin-6 (IL-6), which is one of the key molecules in human immune system, was reported. In Krishnamoorthy et al. [19], a specific receptor for IL-6 was immobilized on the surface of the SAW sensor. Based on the resonant frequency shift due to the IL-6 binding, the detection limit of the SAW sensor was approximately 10^{-18} g. A SAW sensor is also a passive device. The power for operation of the SAW sensor can be delivered by an external device wirelessly which makes the SAW sensor useful for long term biofilm monitoring without a continuous power supply [23]. Furthermore, the SAW sensor can be fabricated using biocompatible materials [24–26]. The combination of extremely high sensitivity, biocompatibility, and low power consumption makes the SAW sensor a unique tool for real time monitoring of bacterial biofilm growth. However, since piezoelectric materials using in the SAW sensor can be dissolved due to long term exposure to liquid, the design of a passivated SAW sensor without loss of sensitivity is critical for biosensing applications [27].

In this work, we have demonstrated a successfully passivated ZnO based SAW sensor for long term biofilm growth monitoring in an animal serum or bacterial growth media. Atomic layer deposition (ALD) was applied for high density and conformal aluminum oxide (Al_2O_3) film deposition to protect the ZnO of the SAW sensor from media. The schematic of the SAW sensor is shown in Fig. 1(a). The SAW sensor was used for the *in vitro* real time study of *E. coli* static biofilm growth in Lysogeny Broth (LB) media and in 10% Fetal Bovine Serum (FBS), the latter of which is the most widely used

serum for mammalian cell culture due to similarities to *in vivo* environments [28].

The remainder of this paper presents the design of the inverted SAW sensor for the targeted mode of the wave and fabrication process. The material and experimental procedures for biofilm detection in the sensor are presented. The results show the biofilm detection using the sensor in consecutive testing both in bacterial growth media and animal serum.

2. Materials and methods

2.1. Design of the SAW sensor

For applications of the SAW sensor in liquid environments, selecting the proper mode of propagation is crucial to prevent severe attenuation of the wave. In a SAW sensor, the surface of the piezoelectric layers is set to a high frequency oscillation governed by the design of the interdigitated transducers (IDT) and the SAW velocity of the piezoelectric material. This no-load oscillation frequency is affected by environmental changes at the surface of the SAW sensor. These effects are observed experimentally as changes in resonant frequency, representing a shift in the SAW phase velocity. However, one of the challenges for biosensor applications is the extremely high attenuation damping of the SAW in liquid environments, when Rayleigh mode waves are generated. In this mode the acoustic wave displacement is perpendicular to the surface and causes significant attenuation of the oscillations in liquid environments. Unlike Rayleigh mode waves, Love mode SAW generation demonstrates displacement planar to the surface and the oscillations are not attenuated in liquid environments [11–15,18–20,29–31]. The generation of Love or Rayleigh mode waves depends on the crystallographic orientation of the piezoelectric film. Therefore, it is critical to deposit piezoelectric material with a specific orientation for generating Love mode SAW [16–22,29–31]. ZnO with a high piezoelectric coefficient is capable of generating very high frequency (GHz) SAW, and it has been shown to grow along the crystallographic orientation that favors Love mode propagation on a SiO_2/Si substrate [19–22]. Love mode waves are predominantly generated with the SAW IDT aligned perpendicular to the *c*-axis of the ZnO film [16–22].

Some critical parameters, such as the SiO_2 thickness, the IDT electrode dimensions, and the ZnO deposition method, had to be considered in the design of a highly sensitive SAW sensor. In order to confine the propagation of the SAW on the surface of the device, a thin film that can prevent acoustic wave loss from the

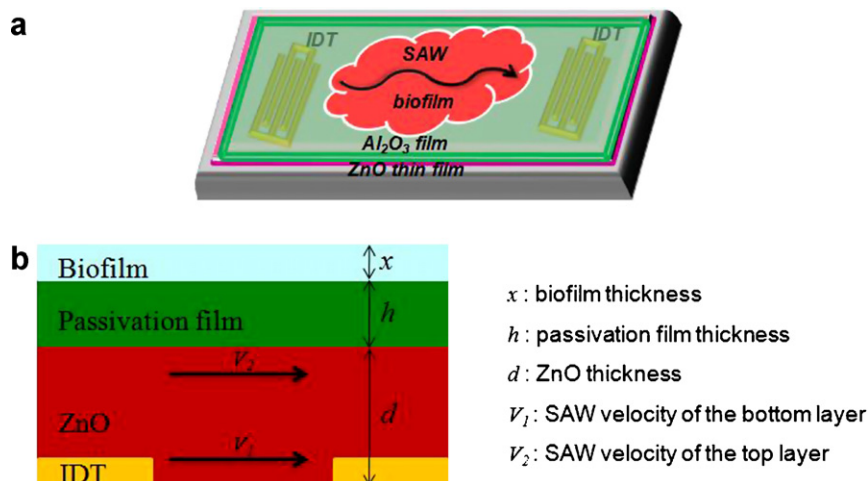


Fig. 1. (a) Schematic of the passivated SAW sensor and (b) a cross sectional view of the inverted passivated SAW sensor.

piezoelectric material to Si substrate was required between ZnO film and Si. SiO₂ was previously shown [15,18] to be an appropriate loss blocking film for thicknesses around 50 nm and was selected in this work. For the best resonance of the SAW at the designed operational frequency, the IDT separation should be equal to the half of the operational wavelength. The acoustic wave velocity for the ZnO thin film used in this work was 4814 m/s, and the operational frequency (401–406 MHz) of the SAW sensor was designed to meet the regulation set by the Federal Communication Commission (FCC) for future biomedical biofilm detection applications [32]. This wavelength (λ) was 12 μm , rendering the electrode separation of the IDT 6 μm ($\lambda/2$). The crystal quality of ZnO film also had to be high for a sensitive SAW sensor. The ZnO film with low impurities and lattice defects was achieved by PLD which has been widely used in metal oxides for high quality film deposition due to stoichiometric deposition with the target material [33] and a relatively simple set-up.

For biofilm detection, it was necessary to invert the standard SAW sensor structure as shown in Fig. 1. In traditional SAW sensor, the IDT is exposed to the liquid environment directly, causing IDT corrosion in long term studies. However, in the inverted SAW sensor, the IDT lifetime is extended because the IDT is patterned under the piezoelectric film. The sensitivity of the Love mode SAW sensor in the top and bottom of piezoelectric films also show the same level of sensitivity for our designed ZnO film thickness (400 nm) based on the Love mode propagation depth [11–14,29].

The material of the IDT, traditionally aluminum in the SAW sensor, can be selected by the acoustic impedance match theory [34]. Potential materials, such as aluminum and gold, were selected and the acoustic power reflective coefficient (R) was calculated based on the theory. The reflective coefficient of the aluminum and gold were 0.058 and 0.012 respectively. The lower reflective coefficient in IDT represents more energy transmission to the piezoelectric material which makes a high sensitive SAW sensor. Therefore, the IDT material was chosen to be gold based on the low R value.

2.2. Selection of passivation film

Since the bare ZnO layer without a passivation film was damaged both in LB media and 10% FBS, selection of the proper material to protect ZnO while considering future biomedical applications is critical to maintain the sensitivity of the sensor. The sensitivity of the passivated SAW sensor is decreased as compared to the unpassivated sensor due to the initial mass loading and dispersion of the wave in the passivation film [12,29,35–40]. To investigate the effect of the added material on the SAW sensitivity in addition to the material selection, we consider only the mass loading effect of the passivation film based on the assumption that the dispersion in the passivation film is minimal due to a much thinner passivation layer (45 nm) as compared to the wavelength of the SAW [35,38,40]. The schematic cross section view of the inverted passivation SAW sensor is shown in Fig. 1(b). The sensitivity of the SAW sensor (S_m^v) is directly proportional to the velocity change due to the mass loading as shown in Eq. (1) [15,18–20].

$$S_m^v = \lim_{\Delta m \rightarrow 0} \frac{1}{\Delta m} \left(\frac{\Delta v}{v_0} \right) \quad (1)$$

where v_0 is the initial velocity of the wave, Δm is the amount of the additional mass, and Δv is the wave velocity changes due to Δm . The SAW velocity (v), shown in Eq. (2), is defined by the shear modulus of the piezoelectric material and local area density based on the one-dimensional acoustic wave Eq. (3) [15,18–20].

$$v = \sqrt{\frac{C}{\rho}} \quad (2)$$

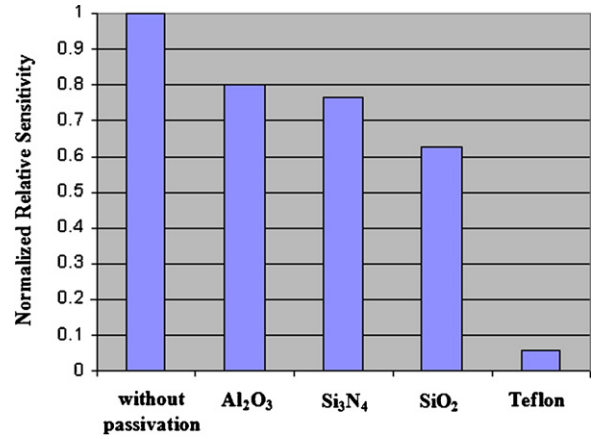


Fig. 2. Normalized sensitivity of the SAW sensor using different passivation materials.

$$\frac{\partial^2 u}{\partial t^2} = \left(\frac{C}{\rho} \right) \frac{\partial^2 u}{\partial y^2} \quad (3)$$

where C is the shear modulus of the surface material, u is the mechanical displacement of the piezoelectric substrate, ρ is material density of the surface, y is the axis of the mechanical displacement propagation, and v is the velocity of the SAW in Eqs. (2) and (3). In order to simplify the modeling of passivation effects on the sensitivity of the SAW sensor, the bacterial growth over the sensor was assumed uniform, so that bacterial mass loading only depended on the thickness of the biofilm. Based on this assumption, the sensitivity of the SAW sensor from Eq. (1) was proportional to the velocity change as biofilm thickness (x) approaches zero as shown in Eq. (4).

$$S_m^v \propto \frac{dv}{dx} \Big|_{x \rightarrow 0} \quad (4)$$

The biofilm formed on the sensor also has a comparatively low shear modulus that can be neglected in the calculation of the total shear modulus of the passivated SAW sensor. The total shear modulus including the ZnO and the passivation film was calculated based on a mechanical spring series connection because the SAW is transferred from ZnO film to the passivation layer sequentially. Based on the assumptions and the total shear modulus calculation, the SAW velocity on a sensor coated with a biofilm was determined by the following Eq. (5).

$$v = \sqrt{\frac{C_{\text{ZnO}}}{\rho_{\text{ZnO}} d} \left(\frac{C_{\text{film}}}{C_{\text{ZnO}} + C_{\text{film}}} \right) \left(\frac{1}{1 + (\rho_{\text{film}} h / \rho_{\text{ZnO}} d) + (\rho_{\text{bac}} x / \rho_{\text{ZnO}} d)} \right)} \quad (5)$$

where C_{film} and C_{ZnO} are the shear moduli of the passivation film and ZnO, ρ_{ZnO} and ρ_{film} are the densities of the ZnO and passivation film, h is the thickness of the passivation film, d is the thickness of the ZnO film, and x is the biofilm thickness. All parameters except the biofilm thickness (x) were determined by selecting potential passivation materials (i.e. Al₂O₃, Si₃N₄, SiO₂ and Teflon) and their thicknesses which were assumed to be 40 nm for all passivation films considered. Potential passivation materials with mechanical properties similar to the ZnO film, such as shear modulus and density, were selected [41,42]. The sensitivity of the SAW sensor with different passivation films was calculated by differentiating Eq. (5) with respect to x , and letting x approach zero, based on Eq. (4). The normalized theoretical sensitivity is shown in Fig. 2. As shown in the figure the lowest degradation in sensitivity is observed for the Al₂O₃ passivation layer with a 0.20 reduction, while Teflon had the maximum degradation at 0.95 reduction.

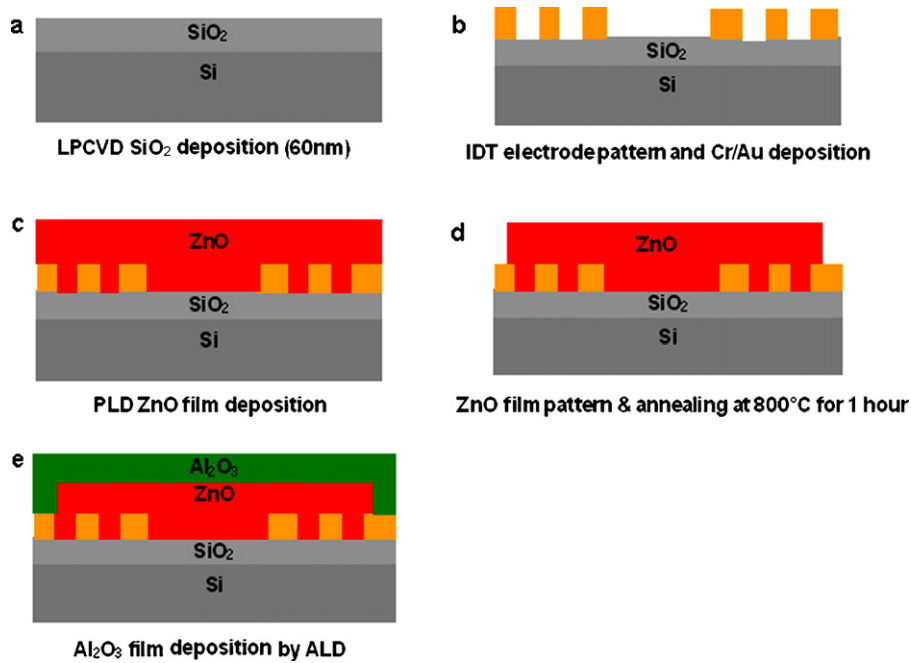


Fig. 3. Overall fabrication process flow.

The application of this fundamental theoretical treatment showed that an Al₂O₃ film was best suited as a passivation layer and it was selected. The thickness of the passivation film (h) in Eq. (5) is critical for our application. The film should be thick enough for effective passivation, but should not be too thick that the added layer causes a significant attenuation both due to mass loading and dispersion of the SAW resulting in substantial loss in sensitivity. The minimum required thickness of Al₂O₃ film (45 nm) was empirically determined. The detailed studies were presented in the film characterization section.

2.3. Fabrication

The fabrication process flow is shown in Fig. 3. A silicon dioxide (SiO₂) layer was deposited on (100)Si substrates by low pressure chemical vapor deposition (LPCVD) as studied in [15,22]. The IDT was patterned using traditional photolithography before depositing the ZnO film. Due to the small feature size of the IDT, including 1 μm, 1.5 μm, and 2 μm wide electrodes, oxygen plasma was used to remove residual photoresist after development. Cr/Au (15 nm/200 nm) as the IDT material was deposited on the wafer by E-beam evaporation, followed by lift-off. The wafer was diced before ZnO deposition by pulsed laser deposition (PLD). Crystalline [001] orientation ZnO films on SiO₂/(100)Si substrates were grown by PLD. The laser deposition system used a KrF excimer laser at a wavelength of 248 nm with pulse duration of 25 ns to ablate a high purity (99.99%) ZnO ceramic target. The ZnO layer was grown at 250 °C with an ambient oxygen partial pressure of $\sim 1.0 \times 10^{-4}$ Torr. After ZnO film deposition, electrical contact pad areas were patterned by photolithography and the ZnO was etched using a solution that consisted of phosphoric acid, acetic acid, and deionized water (1:1:30). The device was annealed at 800 °C for 1 h to increase the resistivity of the ZnO [43]. After annealing, the resistance measured in the IDT increased from 150 Ω to 30–40 MΩ. Finally, the ZnO surface of the SAW sensor was passivated by depositing an Al₂O₃ film using atomic layer deposition (ALD).

2.4. Device characterization and testing

Before the SAW sensor was used to measure biofilm growth, the performance of the passivation film was characterized using an optical microscope to inspect the surface of the ZnO layer after exposure to growth media. The results were used to optimize the film thickness and fabrication process. The sensitivity of the sensor was studied by loading the sensor surface with deionized (DI) water since its viscosity is negligible. After these characterization studies, the sensor response was tested using *E. coli* static biofilm growth.

2.5. Al₂O₃ film characterization

Based on the theoretical modeling calculation presented previously, Al₂O₃ was selected as a passivation film. Al₂O₃ films were deposited to thicknesses of 20–45 nm by ALD to investigate the minimum required thickness for ZnO passivation. SAW sensors with four different thicknesses (20 nm, 30 nm, 40 nm, and 45 nm) of ALD Al₂O₃ film were placed in a LB media bacterial suspension for two days. The surface of the device was inspected using optical microscopy. As shown in Fig. 4, visible ZnO damage was observed when the thickness of ALD Al₂O₃ was thinner than 45 nm.

Based on these experiments, the minimum required thickness of ALD Al₂O₃ film for the passivation of ZnO was 45 nm. Since thicker passivation films caused a high loss of sensitivity due to more initial mass loading, the 45 nm thick Al₂O₃ film was selected to passivate the SAW sensor.

In addition to ALD, other Al₂O₃ film deposition methods were investigated in order to evaluate the dependence of passivation layer performance on the fabrication process. E-beam evaporation and RF-sputtering were used to deposit 45 nm of Al₂O₃ film. However, after two days in an LB media bacterial suspension, these two passivation films were not able to protect the ZnO layer as shown in Fig. 5.

This result can be due to non-uniform or lower density film deposition of E-beam evaporation and RF-sputtering as compared to ALD. Therefore, ALD is a critical fabrication process for effective passivation of the ZnO using Al₂O₃.

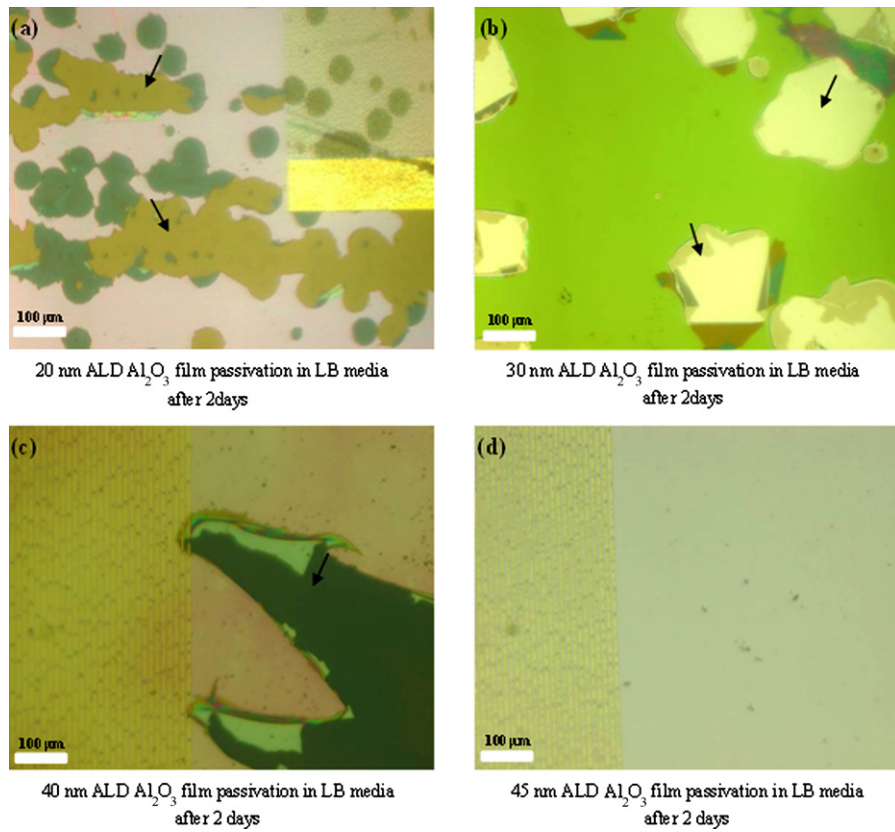


Fig. 4. Optical microscopy images of the SAW sensor passivated by ALD Al_2O_3 with passivation layer thickness of (a) 20 nm, (b) 30 nm, (c) 40 nm (arrows indicate damage to the ZnO) and (d) 45 nm (no ZnO damage).

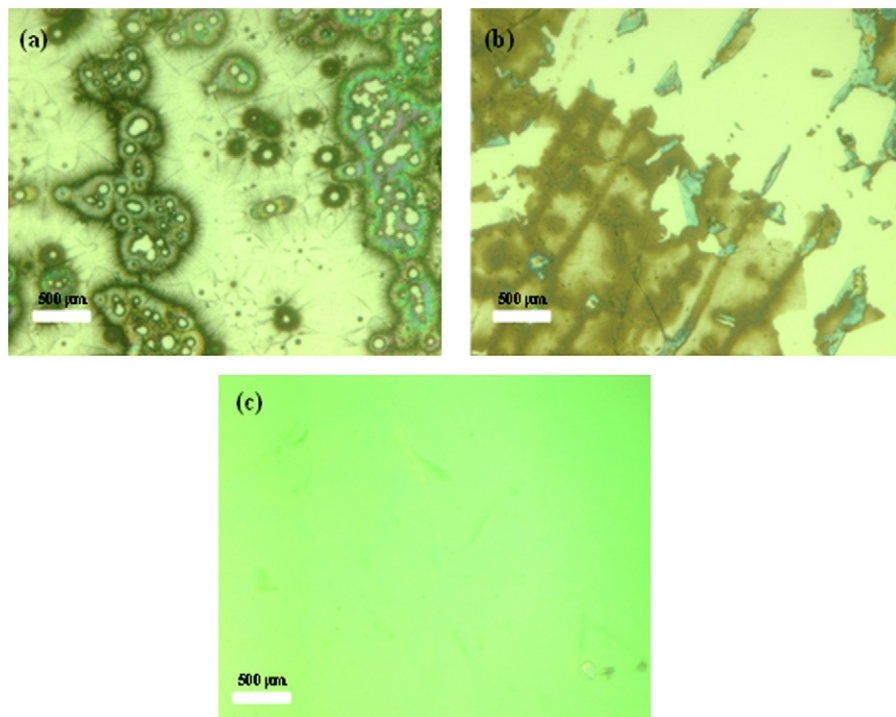


Fig. 5. The optical surface images of the SAW sensor passivated by 45 nm Al_2O_3 film using (a) e-beam evaporation, (b) RF sputtering (dark area is ZnO) and (c) ALD (no ZnO damage) in LB media with the bacterial solution after two days.

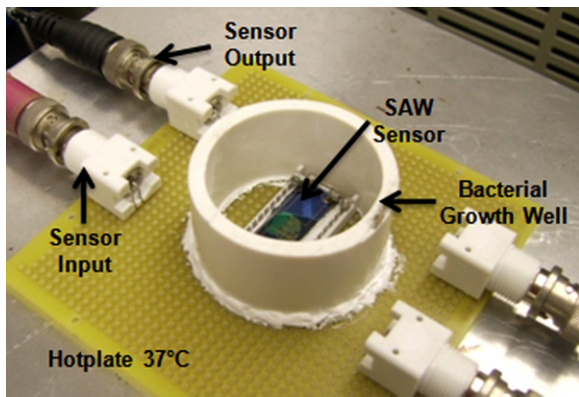


Fig. 6. The sensor package for continuous biofilm growth monitoring.

2.6. Passivated SAW sensor characterization

The mass sensitivity and detection limit of the SAW sensor were studied by loading 10 μl of deionized (DI) water onto the sensor. A volume of 10 μl was used since that was the minimum volume of DI water required to cover the area between the two IDTs of the sensor. By measuring the resonant frequency shift upon mass loading, the sensitivity of the SAW sensor was calculated based on Eqs. (4) and (5). The mass detection limit of the sensor was also calculated using the equipment resolution and the sensitivity.

2.7. Real-time resonant frequency monitoring

For real time resonant frequency monitoring in bacterial biofilm formation experiments, a custom package was designed to enable low impedance BNC cable connections with the network analyzer (HP8510B, Agilent Inc., USA). The device package was composed of a bacterial growth well, which was used to prevent bacterial growth media leakage and localize the bacterial growth, and a chip package connecting the sensor and BNC cables as shown in Fig. 6. The SAW sensor was placed in the bacterial growth well and connected to the BNC connectors by lead soldering on the chip package. The network analyzer was used to sweep a wide range of RF frequencies into the sensor and the device resonant frequency was analyzed using S-parameter analysis. The resonant frequency of the sensor was detected by measuring a low peak of the reflective power ratio (S_{11}) in the network analyzer. Data was collected and saved to a computer every minute using general purpose interface bus (GPIB) communication with the network analyzer.

2.8. Biofilm growth experiments with the SAW sensor

E. coli W3110 was cultured in a shaking incubator for about 16 h. The grown bacterial suspension was diluted with LB media

or 10% FBS to make the initial OD_{600} approximately 0.21–0.23. The total volume of the diluted bacterial suspension in the growth well was 20 ml in experiments with both types of media. The FBS solution was prepared to a 10% concentration by diluting with Dulbecco/Vogt modified Eagle's minimal essential medium (Invitrogen Inc., USA). After filling the bacterial growth well with the diluted bacterial suspension, the well was sealed by paraffin film to prevent evaporation of the media during the experiment. The package was placed on a 37 $^{\circ}\text{C}$ hotplate, and a polystyrene container covered the whole package to reduce the temperature gradient near the test set-up. After each biofilm growth experiment, the sensor was recalibrated using DI water loading. The thickness of biofilm was measured optically by the distance difference between the focal plane of the sensor surface and the focal plane of the top of any accumulated biofilm.

3. Results and discussion

3.1. ZnO film characterization

The generation of Love mode SAW was confirmed by investigating the lattice orientation of the deposited ZnO thin film. X-ray diffraction (XRD) was employed for crystal structure characterization of the ZnO layer after PLD deposition on a SiO_2/Si substrate by measuring the diffraction angle (2θ). The diffraction angles of the X-ray in the ZnO film at 34.25 $^{\circ}$ and 72.25 $^{\circ}$, corresponding to *c*-axis (002) and (004) lattice orientations, were the most intensive reflections in the PLD prepared ZnO film. This *c*-axis orientation of ZnO crystal lattice ((00*L*) direction) was perpendicular to the substrate so that the Love mode of SAW generation was dominant on the surface of the sensor [15–22].

Photoluminescence (PL) spectroscopy was used to investigate the crystal quality of the ZnO film. The peak wavelength of the emitted light was approximately 380 nm, corresponding to the characteristic ZnO bandgap energy (3.3 eV). Therefore, the PL spectroscopy result confirmed that the PLD-prepared ZnO film had a low number of impurities.

3.2. Biofilm cleaning

Consecutive biofilm growth tests using the same device are essential to investigate the reliability and repeatable operation of the SAW sensor. To test the sensor over multiple biofilm growth experiments, surface cleaning after a biofilm growth experiment was crucial for subsequent biofilm growth; cleaning not only sterilized the sensor, but also prevented initial mass loading due to the uncleaned biofilm and the resulting significant loss of sensitivity. Oxygen plasma applied for 30 s at 150 W RF-power was successfully employed to clean any remaining biofilm as shown in Fig. 7.

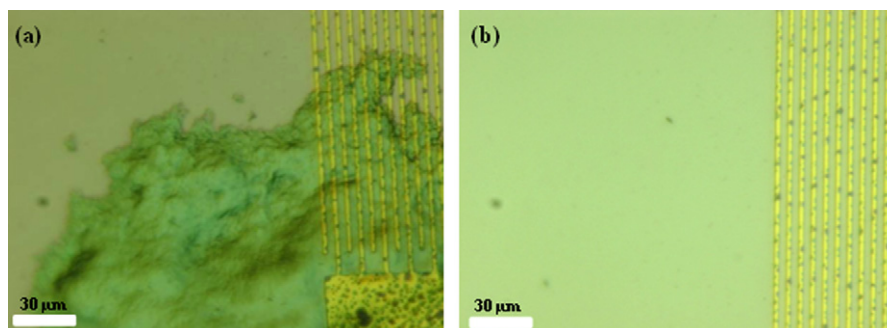


Fig. 7. The optical microscopy images of the surface of the SAW sensor: (a) before biofilm cleaning and (b) after oxygen plasma biofilm cleaning.

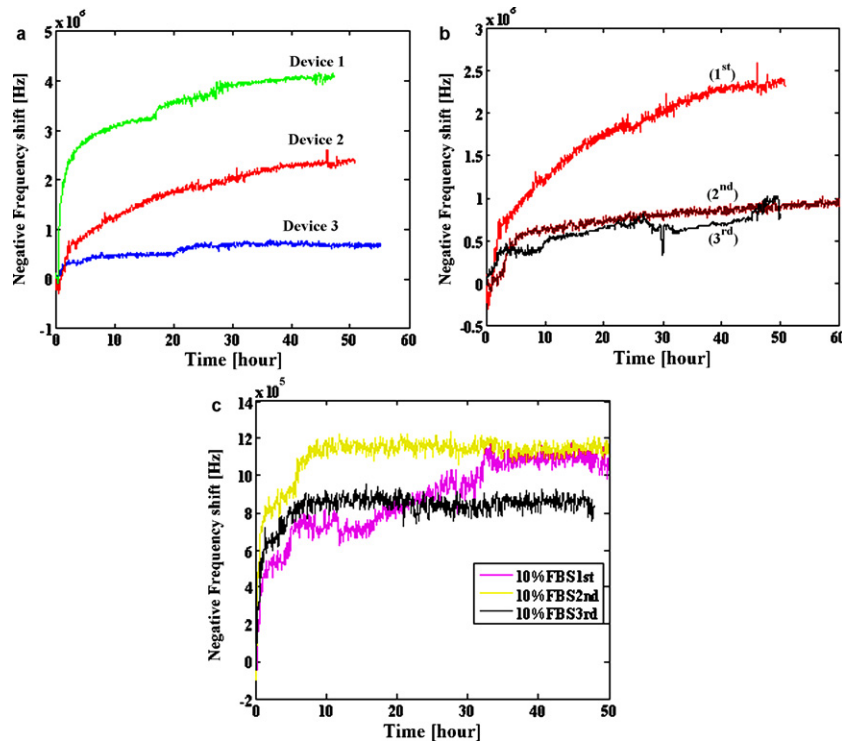


Fig. 8. Resonant frequency shift results in the SAW sensor due to biofilm growth: (a) three newly fabricated SAW sensors (device 1, 2, 3) testing results in LB media biofilm growth experiment, (b) results in three sequential biofilm growth experiments using one device in LB media biofilm growth experiments and (c) resonant frequency shift results in three consecutive biofilm growth experiments using a newly fabricated sensor in 10% FBS (1st, 2nd, and 3rd indicate the order of the experiments).

The 45 nm ALD Al₂O₃ film passivation and oxygen plasma biofilm cleaning method enable our SAW sensor to be reusable over consecutive biofilm growth experiments.

3.3. Sensor sensitivity

The sensitivity and detection limit of the SAW sensor were studied and calculated by loading 10 μ l of DI water on the sensor and monitoring the magnitude of the resonant frequency shift. After loading 10 μ l of DI water, the resonant frequency shift of the SAW sensor was measured to be about 188 kHz by the network analyzer. Hence, the sensitivity of the sensor was 1.88×10^{10} Hz/g. Based on the network analyzer resolution (0.1 Hz), the detection limit of the sensor (resolution/sensitivity) was approximately 5.3 pg. Since the mass of a bacterium is known to be approximately 1 pg [44], this detection limit validates the SAW sensor application for bacterial biofilm monitoring.

3.4. Biofilm growth experiments in the SAW sensor

The resonant frequency shift results of the SAW sensor due to the biofilm growth in LB media and in 10% FBS are shown in Fig. 8. In nature, bacterial growth in batch culture begins with a lag phase where bacteria are not dividing but are actively adapting to the culture conditions. After this period, bacteria divide at a fast rate during the exponential phase of growth. Eventually, once the

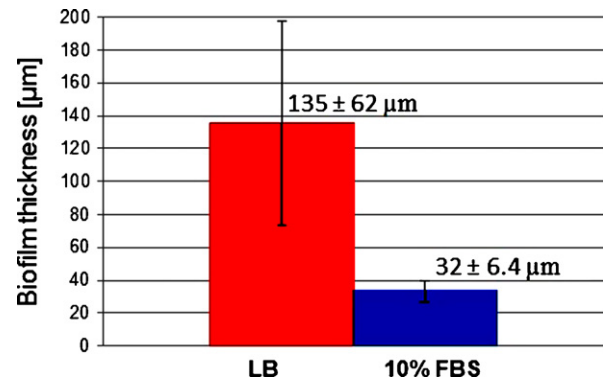


Fig. 9. The averaged biofilm thickness and standard deviation in LB media and in 10% FBS over 30–40 locations measured by optical microscopy. In LB media, the biofilm thickness was $135 \pm 62 \mu\text{m}$ (46% variation). In 10% FBS, it was $32 \pm 6.4 \mu\text{m}$ (20% variation). The large natural variation of the biofilm growth in LB media corresponds to the resonant frequency shift results of the SAW sensor in Fig. 8(a) and (b).

reactor contains a high population density and a limited supply of nutrients, the culture reaches stationary phase [45]. Fig. 8(a) shows the resonant frequency shift results from three newly fabricated devices (device 1, 2, and 3) in the first biofilm growth experiment in LB media. As shown in Fig. 8(a), the frequency shift results of each new sensor show exponential resonant frequency changes

Table 1
Summary of the detection limit of the SAW sensor in sequential biofilm growth experiments.

	Before biofilm experiment	After 1st biofilm growth experiment	After 2nd biofilm growth experiment	After 3rd biofilm growth experiment
Frequency shift due to 10 μ l DI water	185 kHz	157 kHz	141 kHz	143 kHz
Sensitivity	1.85×10^{10} Hz/g	1.57×10^{10} Hz/g	1.41×10^{10} Hz/g	1.43×10^{10} Hz/g
Detection limit	5.4 pg	6.4 pg	7.1 pg	7.0 pg

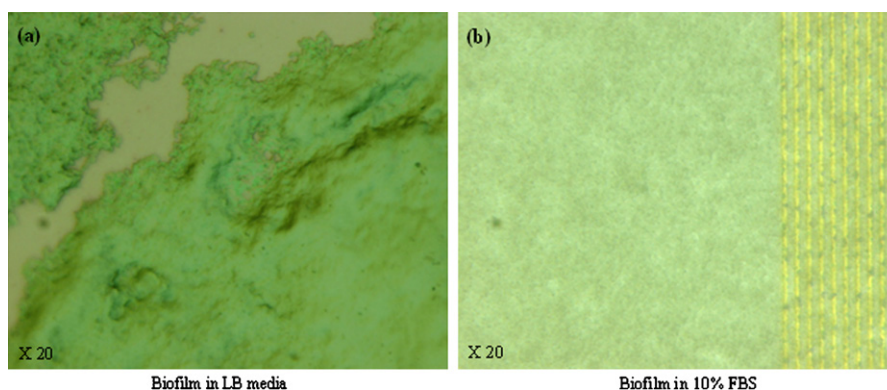


Fig. 10. Microscopy images of the SAW sensor after biofilm growth experiments in (a) LB media and (b) 10% FBS.

at the beginning without the preceding lag phase as compared to the natural bacterial growth trend. These output responses of the SAW sensor can be because the overnight cultured *E. coli* are in a metabolically active state. When active bacteria are diluted to the same growth media, the lag phase may not be observed because bacteria do not have to change their metabolism [46]. However, the stationary phase frequency shifts in LB media biofilm experiments are varied, *i.e.* 0.8 MHz, 2.3 MHz, and 4.1 MHz for each device.

One of the newly fabricated SAW sensors (device 2) after the first experiment was selected and used for two additional sequential biofilm growth experiments in LB media, with the oxygen plasma cleaning applied between uses. The frequency shift results of sequential biofilm growth experiments in LB media as shown in Fig. 8(b) correspond to an exponential growth at the beginning, but the frequency shift observed during stationary phase also varies from 1 MHz to 2.3 MHz. The detection limit of the SAW sensor after each sequential biofilm growth experiment was studied by loading 10 μ l DI water on the sensor. The summary of the calculated detection limit of the SAW sensor for the consecutive experiments is shown in Table 1.

As shown in Table 1, the detection limit of the sensor changed minimally after consecutive biofilm growth experiments, demonstrating excellent sensitivity recovery of the sensor. Therefore, the large variance in the final resonant frequency shift seen in LB media is not a result of sensor degradation, but can be due to non-uniform growth of the biofilm based on the results shown in Fig. 8(a) and (b), and in Table 1. To investigate the biofilm growth variance in LB media and in 10% FBS, twelve test devices were prepared and placed in a bacterial suspension prepared as previously described. The biofilm thickness was measured after two days at 30–40 locations on the devices using an optical microscope. The measured average biofilm thicknesses in LB media and in 10% FBS were 135 μ m and 32 μ m respectively as shown in Fig. 9. The standard deviation of the measured biofilm thickness in LB media (62 μ m, about 46% of the average biofilm thickness) was significantly more than the standard deviation in 10% FBS (6.4 μ m, about 20% of average biofilm thickness).

These results correspond to the large growth variance in LB media measured by the resonant frequency shift of the SAW sensor. Based on these experimental biofilm growth variance results and the sensitivity characterization work as shown in Table 1, the stationary phase resonant frequency shift variation in LB media (Fig. 8(a) and (b)) can be attributed to the natural variation in biofilm growth. The LB media, which is a standard bacterial growth media, is composed of essential materials for *E. coli* growth, such as amino acids, yeast, and NaCl. Thus, the media can provide a favorable environment for biofilm growth. The 10% FBS is mainly composed of diverse blood proteins, such as globular protein and Bovine Serum Albumin (BSA), and has been

widely used as a simulated *in vivo* condition for mammalian cell culture. These composition differences between in LB media and in 10% FBS will cause different bacterial growth rates in each media, contributing to the observed difference in biofilm thickness.

The resonant frequency shift results in 10% FBS biofilm growth experiments are shown in Fig. 8(c). In 10% FBS tests, a newly fabricated SAW sensor was used in three consecutive bacterial biofilm growth experiments, using oxygen plasma cleaning between experiments. As shown in Fig. 8(c), the frequency shift of the sensor also corresponds to exponential growth trend. Furthermore, the variation in the stationary phase in each experiment was only about 0.3 MHz which was much less than variation in LB media (about 3.3 MHz). This smaller difference in the final frequency shifts in 10% FBS compared to the LB media biofilm growth experiments can be due to the more uniform biofilm growth in 10% FBS as shown in Fig. 9. After biofilm growth experiments in each media, the presence of bacterial biofilm on the SAW sensor was confirmed by optical microscopy as shown images in Fig. 10.

As shown in the data, the 45 nm ALD Al_2O_3 passivated SAW sensor was able to measure biofilm growth repeatably using oxygen plasma cleaning between experiments. The final frequency shift results in LB media were more variable than those in 10% FBS since the composition of the LB media was a more favorable environment to *E. coli*, thereby indicating non-uniform biofilm growth in each experiment [47]. The observed SAW sensor outputs in both media followed the same growth trends. Moreover, the 10% FBS results suggest that the SAW sensor can be applied to *in vivo* biofilm detection in the future. Since the FBS is composed of blood proteins and plasma, the serum can be used to mimic an *in vivo* environment. The resonant frequency shift results of the SAW sensor in 10% FBS are more repeatable than results in LB media, rendering reliable operation of the sensor in an *in vivo* environment more likely. The effective passivation of the sensor using an ALD Al_2O_3 film also contributed to reliable sensing in 10% FBS.

4. Conclusions

We have successfully demonstrated a novel ALD Al_2O_3 film passivated SAW sensor for real time biofilm monitoring. A high quality *c*-axis oriented ZnO film was deposited by PLD, and the sensor was effectively passivated by 45 nm of Al_2O_3 film using ALD to prevent ZnO damage in the bacterial growth media and animal serum. For the reliable passivation of the ZnO SAW sensor, ALD was an essential fabrication method based on its highly dense and conformal film deposition capabilities. The SAW sensor can be reused after oxygen plasma cleaning, allowing for consecutive biofilm formation experiments using one sensor. The detection limit of the SAW sensor was approximately 5.3 pg. The resonant frequency shift results of the

SAW sensor followed natural bacterial biofilm growth properties not only in LB media which provided a favorable bacterial growth environment, but also in 10% FBS as a simulated *in vivo* environment. These results validate the application of the SAW sensor for real-time bacterial growth monitoring. This SAW sensor combined with RF wireless communication techniques can be used to detect *in vivo* biofilm growth, which is the groundwork for developing an implantable sensor for early biofilm detection and prevention of major infections.

Acknowledgements

The authors would like to acknowledge the Robert W. Deutsch Foundation and the National Science Foundation (NSF) Emerging Frontiers in Research and Innovation (EFRI) #1042881 and ECS #0823996 for financial support. The authors also would like to thank for the Maryland Nanocenter and Fablab for cleanroom facility support. Finally, the authors acknowledge Dr. Peter Dykstra for useful discussion and consultation.

References

- [1] J.W. Costerton, P.S. Stewart, E.P. Greenberg, Bacterial biofilms: a common cause of persistent infections, *Science* 284 (1999) 1318–1322.
- [2] I.W. Sutherland, Bacterial exopolysaccharides – their nature and production, in: *Surface Carbohydrates of the Prokaryotic Cell*, Academic, London, 1977, pp. 27–96.
- [3] J.W. Costerton, Z. Lewandowski, D.E. Caldwell, D.R. Corber, H.M. Lappin-Scott, Bacterial biofilms in nature and disease, *Annu. Rev. Microbiol.* 41 (1987) 435–506.
- [4] L. Yang, Y. Li, Detection of viable *Salmonella* using microelectrode-based capacitance measurement coupled with immunomagnetic separation, *J. Microbiol. Meth.* 64 (2006) 9–16.
- [5] E. Ghafar-Zadeh, M. Sawan, V.P. Chodavarapu, T. Hosseini-Nia, Bacteria growth monitoring through a differential CMOS capacitive sensor, *IEEE Trans. Bio-Med. Eng.* 4 (4) (2010) 232–238.
- [6] X. Munoz-Berbel, N. Vignes, A.T.A. Jenkins, J. Mas, F.J. Munoz, Impedimetric approach for qualifying low bacteria concentrations based on the changes produced in the electrode–solution interface during the pre-attachment stage, *Biosens. Bioelectron.* 23 (2008) 1540–1546.
- [7] E. Spiller, A. Scholl, R. Alexy, K. Kummerer, G.A. Urban, A sensitive microsystem as biosensor for cell growth monitoring and antibiotic testing, *Sens. Actuators A* 130–131 (2006) 312–321.
- [8] E. Heyduk, T. Heyduk, Fluorescent homogeneous immunosensors for detecting pathogenic bacteria, *Anal. Biochem.* (2010), 396, 298–303.
- [9] B.J. Privett, J.H. Shin, M.H. Schoenfish, Electrochemical sensors, *Anal. Chem.* 82 (2010) 4723–4741.
- [10] M. van Leeuwen, E.E. Krommenhoek, J.J. Heijnen, H. Gardeniers, L.A.M. van der Wielen, W.M. Van Gulik, Aerobic batch cultivation in micro bioreactor with integrated electrochemical sensor array, *Biotechnol. Prog.* 26 (1) (2010) 293–300.
- [11] G.L. Harding, J. Du, P.R. Dencher, D. Barnett, E. Howe, Love wave acoustic immunosensor operating in liquid, *Sens. Actuators A* 61 (1997) 279–286.
- [12] J. Du, G.L. Harding, J.A. Ogilvy, P.R. Dencher, M. Lake, A study of Love-wave acoustic sensors, *Sens. Actuators A* 56 (1996) 211–219.
- [13] J. Du, G.L. Harding, A.F. Collings, P.R. Dencher, An experimental study of Love-wave acoustic sensors operating in liquids, *Sens. Actuators A* 60 (1997) 54–61.
- [14] K.Z. Kourosh, W. Wlodarskia, Y.Y. Chenc, B.N. Fryc, K. Galatsisa, Novel Love mode surface acoustic wave based immunosensors, *Sens. Actuators B* 91 (2003) 143–147.
- [15] S. Krishnamoorthy, A.A. Iliadis, Properties of high sensitivity ZnO surface acoustic wave sensors on SiO₂/(1 0 0) Si substrates, *Solid-State Electron.* 52 (2008) 1710–1716.
- [16] H. Morkoc, U. Ozgur, Zinc Oxide: Fundamentals, Materials, and Device Technology (Chapter 1: General Properties of ZnO), Wiley-VCH Verlag GmbH, Weinheim, 2009.
- [17] R.D. Vispute, et al., High quality crystalline ZnO buffer layers on sapphire (00 1) by pulsed laser deposition for III–V nitrides, *Appl. Phys. Lett.* 70 (20) (1997) 2735–2737.
- [18] S. Krishnamoorthy, A.A. Iliadis, Development of high frequency ZnO/SiO₂/Si Love mode surface acoustic wave devices, *Solid-State Electron.* 50 (2006) 1113–1118.
- [19] S. Krishnamoorthy, A.A. Iliadis, B. Thaleia, G.P. Chrousos, An interleukin-6 ZnO/SiO₂/Si surface acoustic wave biosensor, *Biosens. Bioelectron.* 24 (2008) 313–318.
- [20] M.C. Herrillo, et al., Optimization of SAW sensors with a structure ZnO–SiO₂–Si to detect volatile organic compounds, *Sens. Actuators B* 118 (2006) (2006) 356–361.
- [21] X. Chen, D. Liu, Temperature stability of ZnO-based Love wave biosensor with SiO₂ buffer layer, *Sens. Actuators A* 156 (2009) 317–322.
- [22] X. Chen, D. Liu, J. Chen, G. Wang, The effect of a SiO₂ layer on the performance of a ZnO-based SAW device for high sensitivity biosensor applications, *Smart Mater. Struct.* 18 (2009) 115021.
- [23] A. Springer, R. Weigel, A. Pohl, F. Seifert, Wireless identification and sensing using surface acoustic wave devices, *IEEE ASME Trans. Mechatron.* 9 (1999) 745–756.
- [24] A. Pohl, A review of wireless SAW sensors, *IEEE Trans. Ultrason. Ferroelectr. Freq. Control* 47 (2) (2000) 317–332.
- [25] D.L. Arruda, W.C. Wilson, C. Nguyen, Q.W. Yao, R. Caiazzo, I. Talpasanu, Micro-electrical sensors as emerging platforms for protein biomarker detection in point-of-care diagnostic, *Expert Rev. Mol. Diagn.* 9 (7) (2009) 749–755.
- [26] M. Bisoffi, Detection of viral bioagents using a shear horizontal surface acoustic wave biosensor, *Biosens. Bioelectron.* 23 (2008) 1397–1403.
- [27] Y.Q. Fu, J.K. Luo, X.Y. Du, A.J. Flewitt, Y. Li, G.H. Markx, Recent developments on ZnO films for acoustic wave bio-sensing and microfluidic applications: a review, *Sens. Actuators B – Chem.* 143 (2010) 606–619.
- [28] R.F. Irie, Natural antibody in human serum to neoantigen in human cultured cells grown in fetal bovine serum, *J. Natl. Cancer Inst.* 52 (4) (1974) 1051–1058.
- [29] G. McHale, Generalized concept of shear horizontal acoustic plate mode and Love wave sensors, *Meas. Sci. Technol.* 14 (2003) 1847–1853.
- [30] B.A. Cavic, G.L. Hayward, M. Thompson, Acoustic waves and the study of biochemical macromolecules and cells at the sensor–liquid interface, *Analyst* 124 (1999) 1405–1420.
- [31] B. Drafts, Acoustic wave technology sensors, *IEEE Trans. Microw. Theory* 49 (4) (2001) 795–802.
- [32] <http://wireless.fcc.gov/>.
- [33] D.H. Lowndes, D.B. Geohegan, A.A. Poretzky, D.P. Norton, C.M. Rouleau, Synthesis of novel thin-film materials by pulsed laser deposition, *Science* 273 (1996) 898–903.
- [34] S.E. Voss, J.B. Allen, Measurement of acoustic impedance and reflectance in the human ear canal, *J. Acoust. Soc. Am.* 95 (1) (1994) 372–384.
- [35] B. Jakoby, M.J. Vellekoop, Properties of Love waves: application in sensors, *Smart Mater. Struct.* 6 (1997) 668–679.
- [36] J. Su, Z.B. Kuang, H. Liu, Love wave in ZnO/SiO₂/Si structure with initial stresses, *J. Sound Vib.* 286 (2005) 981–999.
- [37] R.C. Chang, S.Y. Chu, C.S. Hong, Y.T. Chuang, A study of Love wave devices in ZnO/Quartz and ZnO/LiTaO₃ structures, *Thin Solid Films* 498 (2006) 146–151.
- [38] W.C. Shih, H.Y. Su, M.S. Wu, Deposition of ZnO thin films on SiO₂/Si substrate with Al₂O₃ buffer layer by radio frequency magnetron sputtering for high frequency surface acoustic wave devices, *Thin Solid Films* 517 (2009) 3378–3381.
- [39] W.C. Shih, T.L. Wang, L.L. Hsu, Surface acoustic wave properties of aluminum oxide films on lithium niobate, *Thin Solid Films* 518 (2010) 7143–7146.
- [40] J. Du, G.L. Harding, A multilayer structure for Love-mode acoustic sensors, *Sens. Actuators A* 65 (1998) 152–159.
- [41] NIST Property Data Summaries, <http://www.ceramics.nist.gov/srd/summary/emodoo00.htm>.
- [42] <http://www.lenntech.com/teflon.htm>, <http://www.cctplastics.com/teflonall.html>.
- [43] H.-J. Ko, M.-S. Han, Y.-S. Park, Y.-S. Yu, B.-I. Kim, S.S. Kim, Improvement of the quality of ZnO substrates by annealing, *J. Cryst. Growth* 269 (2004) 493–498.
- [44] Davis, Dulbecco, Eisen, Ginsberg, *Bacterial Physiology: Microbiology*, second edition, Harper and Row, Maryland, 1973, pp. 96–97.
- [45] J.V. Straight, D. Ramkrishna, Modeling of bacterial growth under multiplying-limiting conditions. Experiments under carbon- or/and nitrogen-limiting conditions, *Biotechnol. Prog.* 10 (1994) 588–605.
- [46] J.C. Augustin, et al., Significance of inoculum size in the lag time of *Listeria monocytogenes*, *Appl. Environ. Microbiol.* 66 (2000) 1706–1710.
- [47] M.T. Meyer, V. Roy, W.E. Bentley, R. Ghodssi, Development and validation of a microfluidic reactor for biofilm monitoring via optical methods, *J. Micromech. Microeng.* 21 (2011) 054023.

Biographies

Young Wook Kim certified his premedical course from Ulsan Medical School in Korea 2001, and received his B.S. degree in Electrical Engineering from Seoul National University, Korea, in February 2007. He joined the MEMS Sensors and Actuators Lab (MSAL) at the University of Maryland in August 2008 to pursue both his M.S. and Ph.D. degrees in Electrical and Computer Engineering. He received the M.S. degree in February 2011 and is expected to receive his Ph.D. degree in 2013. His research interests are developing an implantable biomedical device.

Saeed E. Sardari is born in Tehran, Iran. He received his bachelor's degree in Biomedical Engineering from National University of Iran in 2001. Mr. Esmaili then attended Georgetown University for some technical courses in mathematics and computer engineering. In 2005, he received a bachelor's degree in Electrical Engineering from the University of Maryland in College Park. He continued his work in device physics and earned his Master's in 2007. His research is focused on growth of high quality oxides on silicon substrates using pulsed laser deposition method. He is currently a Ph.D. candidate.

Mariana T. Meyer received her BS degree in mechanical engineering from Stanford University in June, 2007. She is currently a bioengineering Ph.D. candidate at the University of Maryland, performing research in the MEMS Sensors and Actuators Lab

(MSAL). Her research interests focus on observing and controlling bacterial growth phenomena in microfluidics.

Agis A. Iliadis is the Director of the Semiconductor Nanotechnology Research Laboratory and a member of the Maryland NanoCenter. He received his M.Sc. and Ph.D. degrees in Electrical Engineering, from the Department of Electrical Engineering and Electronics, University of Manchester Institute of Science and Technology (UMIST). His expertise is in the areas of nanotechnology, sensors, semiconductor devices/circuits, and CMOS IC technology. Current research focus is in novel sensors and nanotechnology compatible with CMOS IC technology for developing multi-functionality in CMOS ICs, smart sensor arrays, and nanodevices. His contributions are in the development of self-assembled nanostructures and nanocomposite copolymers on Si CMOS wafers, ZnO and SiC wide band-gap semiconductor devices and technology, gas sensors, heterojunction field effect transistors (HEMTs), SOI MOSFETs, light emitting devices in III–V semiconductors, light emission in Si, ohmic contacts, thin film epitaxial growth, improved metal/semiconductor and oxide/semiconductor interfaces, and electromagnetic interference (EMI) in CMOS integrated circuits.

Hsuan Chen Wu received a Ph.D in the Fischell Department of Bioengineering at the University of Maryland in Dec 2011. He earned a M.S. in life science from Tunghai University, Taiwan, in 2002, and a B.S. in chemical engineering from National Taiwan University in 2000.

William E. Bentley (Ph.D., University of Colorado at Boulder, 1989) is the Robert E. Fischell Distinguished Professor and Chair of the Fischell Department of Bioengineering at the University of Maryland, College Park. He holds joint appointments with the Maryland Technology Enterprise Institute (MTECH) and the Institute for

Bioscience and Biotechnology Research (IBBR). He is a Fellow of the American Academy of Microbiology, American Association for the Advancement of Science, and the American Institute for Medical and Biological Engineering. Dr. Bentley has an outstanding record of technical contributions in metabolic engineering, modeling of genetic circuits, cellular stress responses and *E. coli* protein expression, bioreactor design and optimization, and insect cell and Larvae/Baculovirus expression systems. His work is internationally recognized.

Reza Ghodssi Herbert Rabin Distinguished Professor Reza Ghodssi (Ph.D., University of Wisconsin-Madison 1996) is the Director of the Institute for Systems Research (ISR) and also Director of MEMS Sensors and Actuators Laboratory. Dr. Ghodssi holds a joint appointment with the Department of Electrical and Computer Engineering with affiliation of the Fischell Department of Bioengineering, the Maryland NanoCenter, the University of Maryland Energy Research Center, and the Department of Materials Science and Engineering at the University of Maryland College Park. Dr. Ghodssi's research interests are in the design and development of microfabrication technologies and their applications to micro/nano devices and systems for chemical and biological sensing, small-scale energy conversion and harvesting. Dr. Ghodssi was a chairman of the "MEMS and NEMS Technical Group" at the American Vacuum Society (AVS) from 2002 to 2004 and was a chair of the 9th International Workshop on Micro and Nanotechnology for Power Generation and Energy Conversion Applications (PowerMEMS 2009). Dr. Ghodssi also served as the Americas Technical Program Committee chair of IEEE SENSORS 2010, 2011, and 2012. Dr. Ghodssi has more than 85 scholarly publications, is the co-editor of the *MEMS Materials and Processes Handbook* published in 2011, and is an associate editor for the Journal of Microelectromechanical Systems (JMEMS) and Biomedical Microdevices (BMMD).